Quantum computational calculations and structural investigation of corynan-17-ol, 18, 19-didehydro-10-methoxy, acetate by GC-MS, Fourier Transform Infrared (FT-IR) UV-Vis, NBO, HOMO–LUMO energiesMolecular Docking Studies.

R. Gopathy[1]*A.R. Prabakaran[2] ,P.Rajesh[1,3],A.Subramani[4],P. Kandan[5]

[1,2]Spectrophysics Research Laboratory, Department of Physics, Pachaiyappa's College, Chennai 600030,Tamil NaduIndia.
[3,4]Department of Physics, Apollo Arts and Science College, Kanchipuram,603105, Tamil Nadu,India.
[5]Department of Mathematics, Annamalai University, Chidambaram 608 002, Tamil NaduIndia.

***Abstract*:** This study aimed to evaluate the isolated from leaves of corynan-17-ol,18,19-didehydro-10-methoxy, acetate and its structure was characterized using, Gas chromatography mass spectrometry [GC–MS], fourier transform infrared spectroscopy [FT-IR] and UV–Vis spectroscopy. Corynan-17-ol, 18, 19-didehydro-10-methoxy, acetate of isolated compound. Density functional theory calculations are carried out for the first time for geometric, electronic and spectroscopic properties of (corynan-17-ol, 18, 19-didehydro-10-methoxy, acetate).Atomic charges, donor-acceptor NBO hyper conjugative interactions, Ionization potential and electron affinities, HOMO-LUMO gap and molecular electrostatic potential were also computed at B3LYP/6-311++G(d,p)level.

Keywords: Molecular Docking, NBO, FT-IR

1. Introduction

Chemically, quinolizine derivatives contains vinyl substituted in third position and ester group in fourth position and finally 9-methoxy indole are attached in the [2, 3 a] position of the quinolizine ring. The overall chemical formula of this compound is $C_{22}H_{28}N_2O_3$. From the structural point of view quinolizine a hypothetical structure the N atom substituted between the two six member cyclic rings (heterocyclic). Carmen and et. al synthesized quinolizine derivatives by the intermolecular mannich reaction. In these connectivity is not steroselctive, under the thermodynamics condition the main product are the transquinolizine but in the case kinetic condition give cis stereochemistry the relative position C-4 and C-10 hydrogens. Quinolizine derivatives is one of the most important heterocyclic medicinal compound possess broad range of biological system such as antimalaria, anti-HIV, antiviral, antituberculosis and anti-inflammatory[1]. As per the structure relationship activity of chiral based quinazoline derivatives possess significant effect in the biological system Masanori Tobeet. al [ref: Structure±Activity Relationships of Quinazoline Derivatives: Bioorganic & Medicinal Chemistry Letters 11 (2001) 545±548].

Its chemical name corynan-17-ol, 18, 19-didehydro-10-methoxy, acetate is main reason for the medicinal properties of Cassia auriculata (Family; Caesalpinaceae) is a common asian beverage and medicinal plant that is used in traditional medicine to treat diseases namely, helminthes infection, eye diseases, diabetes and skin problems[2]. In this study, the developed combined spectroscopic and computational approach is demonstrated to be a powerful tool to characterize these effects at the molecular level with high spectroscopic precision. This present investigation were undertaken to study the compounds were identified through GC-MS analysis of MC extract. ,UV–Vis spectroscopy (UV– Vis), fourier transform infrared spectroscopy (FT-IR), geometrical frame work review, electronic properties such as band gap, frontier molecular orbitals energies were also simulated for the first time; however no comparison could be made with the experiment ,have been carried out on corynan-17-ol, 18, 19-didehydro-10-methoxy, acetate .

2. Experimental Details

2.1. Isolation of Compound From Cassia Auriculata Leaves And Extraction And Initial Fractionations.

The collected plant materials of Cassia auriculata were air-dried, ground and extracted at room temperature with in a Soxhlet apparatus using n-hexane, CH2Cl2, EtOl and MeOH successively to give 18.5, 10.2, 2.5 and 91.0 g of extract respectively.

2.2. GCMS

GC-MS analysis isolates the six different compounds of medicinal importance from the methanol extract of the Cassia auriculata. The GC-MS spectrum and peak fragmentation are shown in **(Fig 1)**. GC-MS plays a key role in the analysis of known and unknown components of the plant origin. GC-MS ionizes compound and measures their mass numbers. The use of mass spectrometry (MS) is most cases coupled to an appropriate separation technique as gas chromatography. GC-MS analysis of phyto constituents in plants gives a clear picture of the pharmaceutical value of the plant.[3]. The result of the GC-MS analysis led to the identification of number of compounds peak from GC fractions of the Laq extract of corynan-17-ol,18,19-didehydro-10-methoxy, acetate .

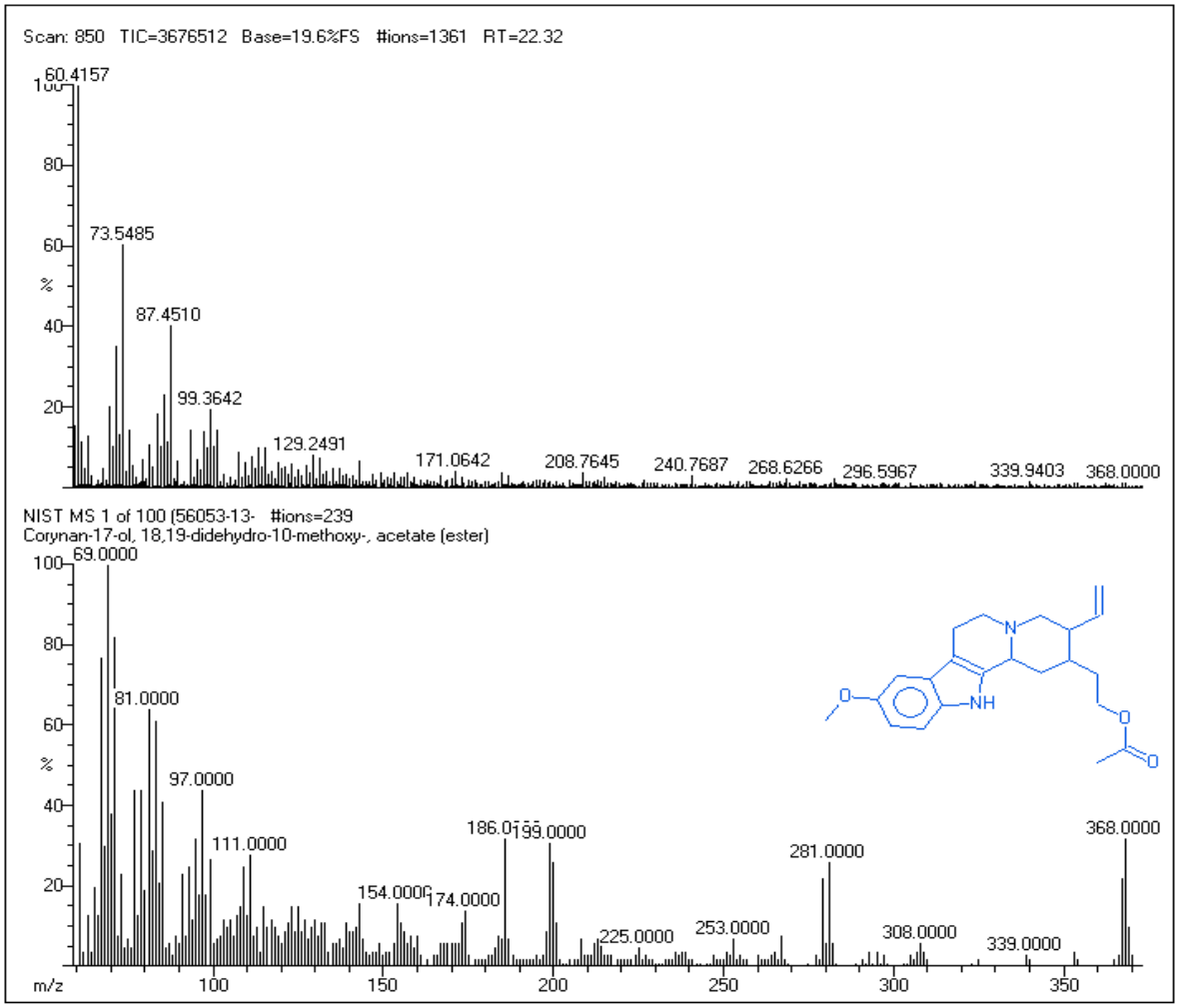

Fig. 1. GCMS of corynan-17-ol, 18, 19-didehydro-10-methoxy, acetate.

2.3. Fourier Transform–Infrared Spectroscopy (FT–IR)

The FT-IR spectrum was recorded in the spectral range 4000-400 cm^{-1} with a spectral resolution of 4 cm^{-1} by using Bruker TENSOR 27 FT–IR (Fourier transform–infrared spectroscopy spectrometer).

2.4. UV–Visible Spectroscopy

The UV-Visible absorption spectrum of genistein was recorded in a methanol solvent with a Varian Cary 50, UV–Visible spectrophotometer. The spectral region was 200–400 nm.

3. Computational Details

All calculations presented in this study were performed by using Gaussian 09 software .The computational details are given in the supporting information, which have used for the calculation in vibrational spectrum, PED, NBO, UV-Vis,MEP , Mulliken population analysis and HOMO-LUMO analysis were performed using Gaussian 09 software by B3LYP method at 6-311++G(d,p) level [4].

4. Molecular Geometry and Structural Properties

Three dimensional optimized structures of corynan-17-ol,18,19-didehydro-10-methoxy, acetate were also shown in Fig.2.The role of optimized structural parameters bond length, bond angle and dihedral angle for the thermodynamically preferred geometry of the corynan-17-ol,18,19-didehydro-10-methoxy, acetate has greater influences upon determining molecular properties. The calculated geometric parameters of the title molecule corynan-17-ol,18,19-didehydro-10-methoxy, acetate has own nearly 58 bond length and107 bond angle are presented in Table 1.The highest value of energy difference found for the rotation of C_{13}-C_{14} (1.5529)bond suggests that the deviation from the minimum energy structure is the least likely for the rotation of this single bond. In the case of rotation of N_{17}-H_{46} (1.0059)bonds, the rotational energy barriers are the lowest.

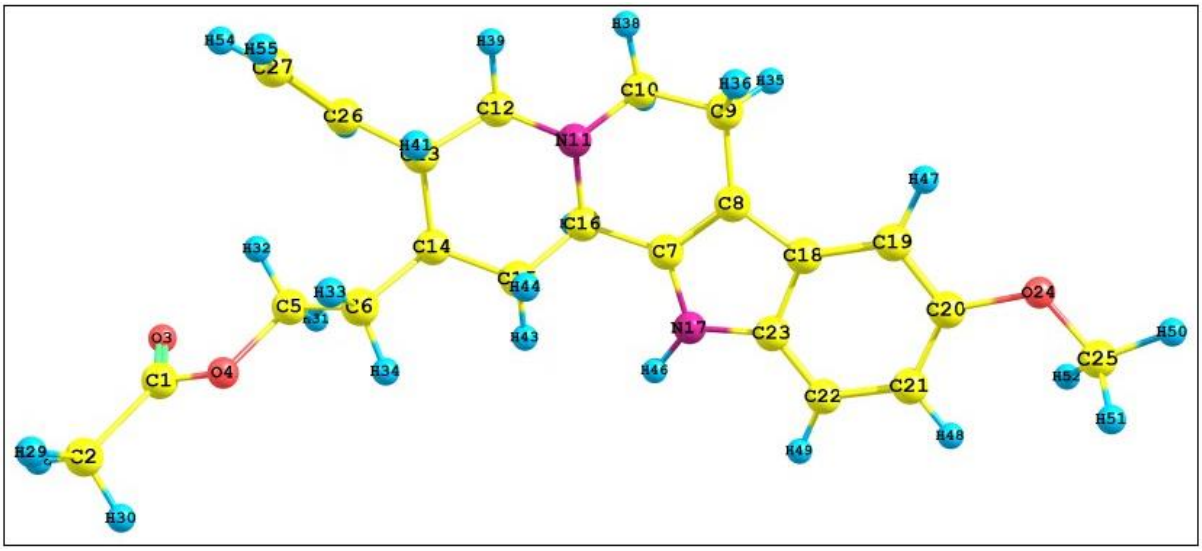

Fig 2. Optimized Structure of Corynan-17-Ol, 18, 19-Didehydro-10-Methoxy, Acetate.

Table 1 Optimized geometric parameters of corynan-17-ol, 18, 19-didehydro-10-methoxy, acetate obtained by B3LYP method.

Bond length	B3LYP/6-31G++ (d,p)	Bond angle	B3LYP/6-31++G (d,p)
C_1-C_2	1.5108	C_7-C_8-C_9	121.2554
C_1-O_3	1.2118	C_7-C_8-C_{18}	107.1457
C_1-O_4	1.3526	C_9-C_8-C_{18}	131.5927
C_2-H_{28}	1.0894	C_8-C_9-C_{10}	108.9738
C_2-H_{29}	1.0941	C_8-C_9-H_{35}	111.2182
C_2-H_{30}	1.0937	C_8-C_9-H_{36}	111.1298
O_4-C_5	1.4473	C_8-C_9-H_{36}	111.1298
C_5-C_6	1.5226	C_{10}-C_9-H_{35}	109.2714
C_5-H_{31}	1.0957	C_{10}-C_9-H_{36}	109.4624
C_5-H_{32}	1.0916	H_{35}-C_9-H_{36}	106.7438
C_6-C_{14}	1.5455	C_9-C_{10}-N_{11}	110.9056
C_6-H_{33}	1.0969	C_9-C_{10}-H_{37}	109.4387
C_6-H_{34}	1.097	C_9-C_{10}-H_{38}	110.0601
C_7-C_8	1.3706	N_{11}-C_{10}-H_{37}	111.4743
C_7-C_{16}	1.501	N_{11}-C_{10}-H_{38}	107.802
C_7-N_{17}	1.3839	H_{37}-C_{10}-H_{38}	107.0712
C_8-C_9	1.4984	C_{10}-N_{11}-C_{12}	112.8723
C_8-C_{18}	1.4391	C_{10}-N_{11}-C_{16}	113.1351
C_9-C_{10}	1.5356	C_{12}-N_{11}-C_{16}	110.7193
C_9-H_{35}	1.0974	N_{11}-C_{12}-C_{13}	111.7623
C_9-H_{36}	1.0986	N_{11}-C_{12}-H_{39}	108.4185
C_{10}-N_{11}	1.4674	N_{11}-C_{12}-H_{40}	111.9588
C_{10}-H_{37}	1.1075	C_{13}-C_{12}-H_{39}	108.6366
C_{10}-H_{38}	1.0948	C_{13}-C_{12}-H_{40}	109.1639
N_{11}-C_{12}	1.4576	H_{39}-C_{12}-H_{40}	106.7201
N_{11}-C_{16}	1.4691	C_{12}-C_{13}-C_{14}	110.1336
C_{12}-C_{13}	1.5446	C_{12}-C_{13}-C_{26}	109.3161
C_{12}-H_{39}	1.0947	C_{12}-C_{13}-H_{41}	106.9716
C_{12}-H_{40}	1.1107	C_{14}-C_{13}-C_{26}	113.702
C_{13}-C_{14}	1.5529	C_{14}-C_{13}-H_{41}	107.7129
C_{13}-C_{26}	1.5068	C_{26}-C_{13}-H_{41}	108.7677
C_{13}-H_{41}	1.0983	C_6-C_{14}-C_{13}	113.9215
C_{14}-C_{15}	1.5404	C_6-C_{14}-C_{15}	110.0918
C_{14}-H_{42}	1.1024	C_6-C_{14}-H_{42}	108.547
C_{15}-C_{16}	1.5371	C_{13}-C_{14}-C_{15}	109.3261
C_{15}-H_{43}	1.0977	C_{13}-C_{14}-H_{42}	107.4674
C_{15}-H_{44}	1.0966	C_{15}-$C1_4$-H_{42}	107.2413
C_{16}-H_{45}	1.1145	C_{14}-C_{15}-C_{16}	112.3339
N_{17}-C_{23}	1.3866	C_{14}-C_{15}-H_{43}	108.7847
N_{17}-H_{46}	1.0059	C_{14}-C_{15}-H_{44}	110.0624
C_{18}-C_{19}	1.4007	C_{16}-C_{15}-H_{43}	109.7637
C_{18}-C_{23}	1.4247	C_{16}-C_{15}-H_{44}	108.495

C_{19}-C_{20}	1.3946	H_{43}-C_{15}-H_{44}	107.2746
C_{19}-H_{47}	1.0851	C_7-C_{16}-N_{11}	108.6399
C_{20}-C_{21}	1.4112	C_7-C_{16}-C_{15}	113.3827
C_{20}-O_{24}	1.375	C_7-C_{16}-H_{45}	108.4413
C_{21}-C_{22}	1.3948	N_{11}-C_{16}-C_{15}	108.9588
C_{21}-H_{48}	1.0829	N_{11}-C_{16}-H_{45}	110.0734
C_{22}-C_{23}	1.3921	C_{15}-C_{16}-H_{45}	107.3203
C_{22}-H_{49}	1.0864	C_7-N_{17}-H_{23}	108.8093
O_{24}-C_{25}	1.4146	C_7-N_{17}-H_{46}	125.8088
C_{25}-H_{50}	1.0916	H_{23}-N_{17}-H_{46}	125.8088
C_{25}-H_{51}	1.0985	C_8-C_{18}-C_{19}	134.0521
C_{25}-H_{52}	1.0985	C_8-C_{18}-C_{23}	106.6846
C_{26}-C_{27}	1.3339	C_{19}-C_{18}-C_{23}	119.2623
C_{26}-H_{53}	1.0917	C_{18}-C_{19}-C_{20}	119.1246
C_{27}-H_{54}	1.0859	C_{18}-C_{19}-H_{47}	121.9695
C_{27}-H_{55}	1.0875	C_{20}-C_{19}-H_{47}	118.9058
C_2-C_1-O_3	125.5123	C_{19}-C_{20}-C_{21}	120.9467
C_2-C_1-O_4	110.8369	C_{19}-C_{20}-C_{24}	115.4214
O_3-C_1-O_4	123.6508	C_{21}-C_{20}-C_{24}	123.6319
C_1-C_2-H_{28}	109.4264	C_{20}-C_{21}-C_{22}	120.6679
C_1-C_2-H_{29}	109.9719	C_{20}-C_{21}-H_{48}	120.488
C_1-C_2-H_{30}	110.197	C_{22}-C_{21}-H_{48}	118.844
H_{28}-C_2-H_{29}	109.8591	C_{21}-C_{22}-C_{23}	118.3612
H_{28}-C_2-H_{30}	110.0485	C_{21}-C_{22}-H_{49}	120.1503
H_{29}-C_2-H_{30}	107.3142	C_{23}-C_{22}-H_{49}	121.4885
C_1-O_4-C_5	115.7797	N_{11}-C_{23}-C_{18}	107.4694
O_4-C_5-C_6	107.0443	N_{11}-C_{23}-C_{22}	130.8933
O_4-C_5-H_{31}	108.8328	C_{18}-C_{23}-C_{22}	121.6372
O_4-C_5-H_{32}	108.9734	C_{20}-O_{24}-C_{25}	118.4091
C_6-C_5-H_{31}	111.541	O_{24}-C_{25}-H_{50}	106.0902
C_6-C_5-H_{32}	112.5865	O_{24}-C_{25}-H_{51}	111.9865
H_{31}-C_5-H_{32}	107.788	O_{24}-C_{25}-H_{52}	111.9782
C_5-C_6-C_{14}	114.397	H_{50}-C_{25}-H_{51}	108.9485
C_5-C_6-H_{33}	109.3126	H_{50}-C_{25}-H_{52}	108.9546
C_5-C_6-H_{34}	107.4296	H_{51}-C_{25}-H_{52}	108.7819
C_{14}-C_6-H_{33}	109.9119	C_{13}-C_{26}-C_{27}	125.18052
C_{14}-C_6-H_{34}	109.1765	C_{13}-C_{26}-H_{53}	115.8419
H_{33}-C_6-H_{34}	106.2735	C_{13}-C_6-H_{53}	118.9421
C_8-C_7-C_{16}	125.4218	C_{26}-C_{27}-H_{54}	1217483
C_8-C_7-N_{17}	109.8877	C_{26}-C_{27}-H_{55}	121.6058
C_{16}-C_7-N_{17}	124.6713	H_{54}-C_{27}-H_{55}	116.6458

5. Vibrational Wavenumbers Assignments (FT-IR Spectral Analysis)

The maximum number of potentially active observable fundamentals of a non-linear molecule, which contains N atoms, is equal to (3N-6) apart from three translational and three rotational degrees of freedom. The title molecule consists of 55 atoms and belongs to C_1 point group symmetry.

C-H, CH_2, CH_3Vibrations

The C-H stretching vibrations are normally observed in the region 3100-3000 cm^{-1}.The vibration observed at 3073,3030 cm^{-1} is due to C–H stretching. The CH_3 asymmetric stretching vibrations are expected in the range 2925–3000 cm^{-1} and the CH_3 vibrations observed and assigned at 2998, 3005 cm^{-1} in the FT-IR spectrum as seen in Fig. 3. The CH_2 asymmetric vibrations are usually observed in the region 3100 – 3000 cm^{-1} respectively. The vibration observed at 3084 cm^{-1} is due to C–H stretching are listed in Table 2[5].

C-C Vibrations

The C-C stretching vibrations, known as stretching usually occur in the region 1650-1400 cm-1[6].In the present work, the wavenumbers observed in the FT-IR spectrum at 1501 and 1400 cm^{-1} are assigned to C–C stretching vibrations are listed in Table 2.The bands at 620 and 354 cm^{-1} in FT-IR spectra are assigned to the C–C–C deformation of the phenyl ring.

C=O and C-O Vibrations

Very strong bands observed at 1079 cm^{-1} in corynan-17-ol, 18, 19-didehydro-10-methoxy, acetate, 1080 cm^{-1} respectively are assigned C–O stretching vibration. The C=O stretch of carboxylic acids in identical to the C=O stretch in ketones, which is expected in the region1740-1660 cm-1[7].The title compound C= O mode has been seen as a strong band at 1735 cm^{-1} in the FT-IR spectrum as seen in Fig. 3.

C-N Vibrations

The assigned C–N stretching absorption in the region 1250–1020cm^{-1}.The bands observed at 1122 cm^{-1} in FT-IR spectra had been assigned to C–N stretching vibrations of corynan-17-ol, 18, 19-didehydro-10-methoxy, acetate The C-N stretching and C-N bending vibrations of a nitro group occur near 970 cm^{-1}, and 792 cm^{-1}, respectively[8].Theoretical calculations which are also in good agreement with the experimental data.

.

N-H Vibrations

The N–H stretching vibrations occur in the region 3550–3300 cm^{-1}.In the present investigation the N–H stretching vibrations have been found in FT-IR at 3663 cm^{-1} with 100% of PED contribution are listed in Table 2.The calculated value of this mode of vibration is obtainedas 3662 cm^{-1} in B3LYP/6-311++G(d,p). These observations agreed well with the earlier reports [9,10].

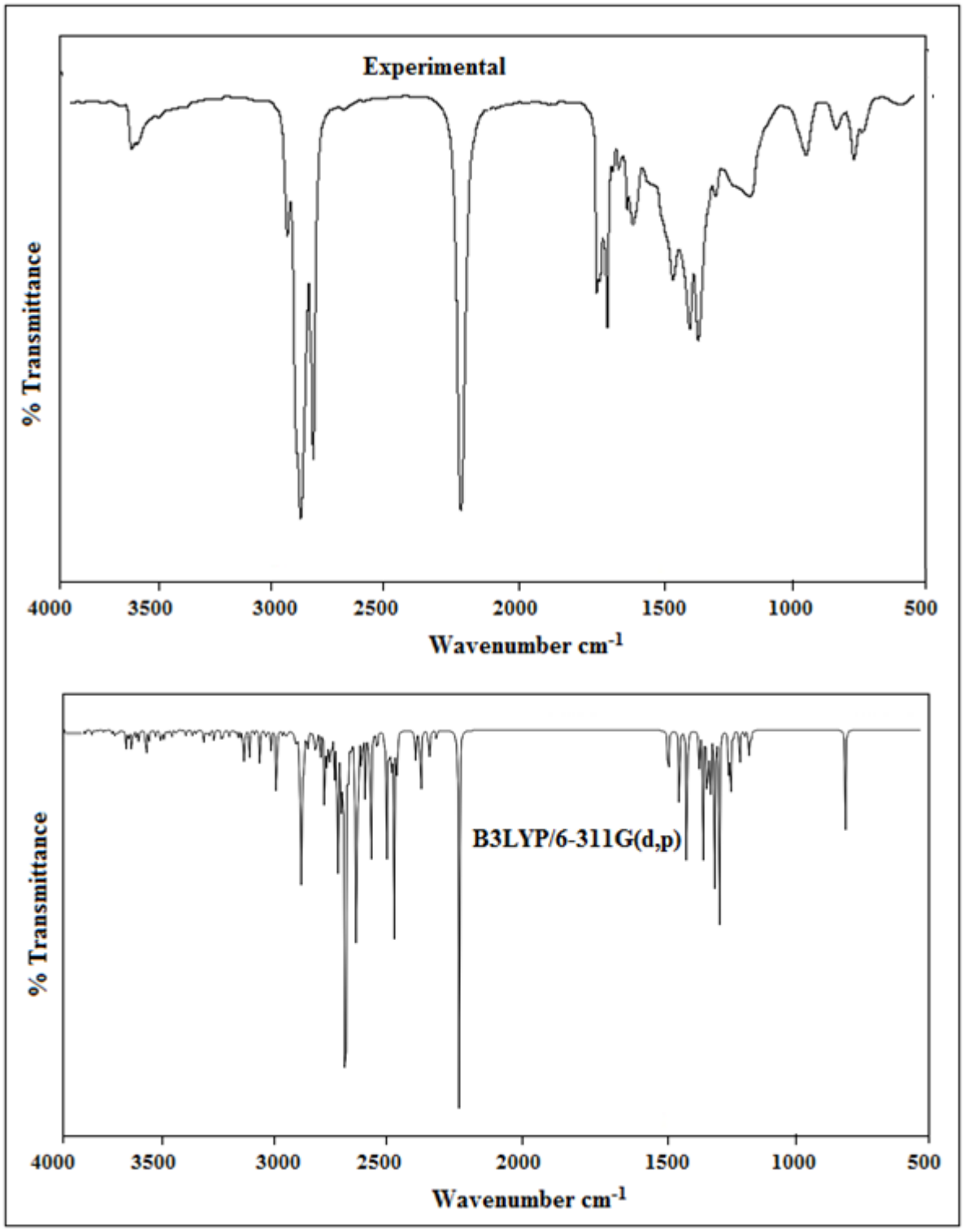

Fig. 3. Observed and Calculated FT-IR spectrum of corynan-17-ol, 18, 19-didehydro-10-methoxy, acetate.

Table 2: FT-IR Computed Vibrational Band Assignment of corynan-17-ol, 18, 19-didehydro-10-methoxy, acetate.

Calculated B3LYP/6-31++G(d,p)	Exp	Vibrational Assignments+(PED)
3662	3663	υNH(100)
3235	3230	υCH(95)
3226	3220	υCH(99)
3206	-	υCH(99)
3184	-	υCH(75)
3151	-	υCH(83)
3139	-	υCH(83)
3137	-	υCH(74)
3128	-	υCH(96)
3084	-	υCH_2(91)
3080	3073	υCH_2(91)
3066	-	υCH(90)
3061	-	υCH(80)
3060	-	υCH(86)
3041	-	υCH(90)
3037	-	υCH(92)
3030	3030	υCH(85)
3023	-	υCH(92)
3005	2998	υCH_3(91)
2988	-	υCH(97)
2928	-	υCH(96)
2891	-	υCH(96)
2838	2829	υCH(98)
1798	-	υCC(13)
1722	1735	υCO(72)
1778	-	δHCH(61)+ δHCN(10)+ τHCOC(12)
1531	-	δHCO(65)+ δHCH(11)
1521	-	δHCH(80)
1507	1501	υCC(10)+ δHCH(41)+ τHCOC(62)
1497	-	υCC(43)
1494	-	δHCH(83)
1487	-	δHCH(84)
1481	1474	δHCH(23)+ τHCCO(59)
1419	-	υCC(43)
1406	1400	υCC(19)
1401	-	δHCC(73)
1393	-	τHCCO(42)
1376	1376	τHCOC(57)
1361	-	δHCO(39)
1346	-	δHCO(47)
1307	-	δHCO(42)
1297	1289	δHCC(61)
1233	-	δHCO(61)
1230	-	δHCC(48)
1216	-	τHCCC(36)
1142	1140	υCC(56)
1135	-	υCC(34)
1130	1122	δHNC(12)
1098	-	υCC(49)
1080	1079	υCO(51)
1070	-	υCC(31)+ τHCOC(19)
1059	-	υCC(44)
1026	-	δHCO(53)
960	970	δHCC(10)+ τHCNC(14)
948	-	δHCC(72)
900	-	υCC(12)
811	-	υOC(25)
792	-	δHNC(23)

776	-	τHCOC(37)
763	-	δHCC(49)
687	-	δHCC(22)
631	620	τHCCC(46)
622	-	τHCCC(14)
597	-	δHCC(57)
436	-	δHCC(29)
415	-	δHCC(34)
395	-	δCOC(42)
392	-	δCOC(16)
368	354	τHCCC(71)
323	-	τHCCC(13)
282	-	τHCCC(10)
267	-	δHCC(16)
224	-	τHCNC(15)
244	-	τHCCC(16)
189	-	τHCCO(35)
172	-	τHCCC(20)
149	-	τHCOC(27)
106	-	τHCCC(13)
67	-	τHCCO(15)
54	-	τHCCO(43)
49	-	τHCOC(26)
29	-	τHCCO(52)

6. Mulliken Population Analysis

In both Mulliken charge using B3LYP/6- 311++G(d,p), the H_{46} and H_{29}atoms showed the highest positive value (0.0247764 and 0.046241, respectively) due to its attachment to the electronegative oxygen atom. The natural charges of all hydrogen atoms are positive with higher values than Mulliken charges.Carbon atom having more positive charge (05865) compared with all other atoms, due to that more protons are occupied the perchlorate anion moiety. Mulliken population analysis (MPA) of corynan-17-ol, 18, 19-didehydro-10-methoxy, acetate molecule has been carried out at B3LYP/6-311++G(d,p) levels. Table 3 shows the partial charges located on the various atoms of the corynan-17-ol, 18, 19-didehydro-10-methoxy, acetate molecule. As evident fromTable 3**,** electronegative atomslike nitrogen and oxygen always possess negative charge[11]. Hydrogen atoms bear electropositive charge irrespective of their position in the molecule. However, carbon atoms assume both positive and negative charge according to their positions in the molecule.

Table 3: Mulliken Charges of corynan-17-ol, 18, 19-didehydro-10-methoxy, acetate.

Atoms	B3LYP/6-31G++(d,P)	Atoms	B3LYP/6-31G++(d,P)
C_1	0.586537	H_{28}	0.137058
C_2	-0.383983	H_{29}	0.149672
O_3	-0.477402	H_{30}	0.138941
O_4	-0.470121	H_{31}	0.102462
C_5	0.059395	H_{32}	0.126371
C_6	-0.201130	H_{33}	0.116899
C_7	0.267389	H_{34}	0.102187
C_8	0.018104	H_{35}	0.095985
C_9	-0.225640	H_{36}	0.120906
C_{10}	-0.039170	H_{37}	0.071543
N_{11}	-0.450913	H_{38}	0.094556
C_{12}	-0.007842	H_{39}	0.106162
C_{13}	-0.099334	H_{40}	0.058308
C_{14}	-0.075341	H_{41}	0.101808
C_{15}	-0.178251	H_{42}	0.072076
C_{16}	0.060478	H_{43}	0.071628
N_{17}	-0.698657	H_{44}	0.120341
C_{18}	0.047474	H_{45}	0.066171
C_{19}	-0.189992	H_{46}	0.247764
C_{20}	0.344949	H_{47}	0.087014

C_{21}	-0.151401	H_{48}	0.075854
C_{22}	-0.123881	H_{49}	0.071865
C_{23}	0.305498	H_{50}	0.120972
O_{24}	-0.527252	H_{51}	0.111459
C_{25}	-0.071831	H_{52}	0.097237
C_{26}	-0.026732	H_{53}	0.079758
C_{27}	-0.244942	H_{54}	0.102656
		H_{55}	0.106287

7. MEP

Electrostatic potential maps illustrate the charge distributions of molecules three dimensionally. These maps allow us to visualise variably charged regions of a molecule. Knowledge of the charge distributions can be used to determine how molecules interact with one another. In the majority of the MEPs, while the maximum negative region(-0.0804) which preferred site for electrophilic attack indications as a red color, the maximum positive region which preferred site for nucleophilic attack symptoms as blue color. The importance of MEPs lies in the fact that it simultaneously displays molecular size, shape, as well as positive regions(0.0326) in terms of color grad, is very useful in research of molecular structure with its physicochemical relationshipare shown in Fig. 4[12].

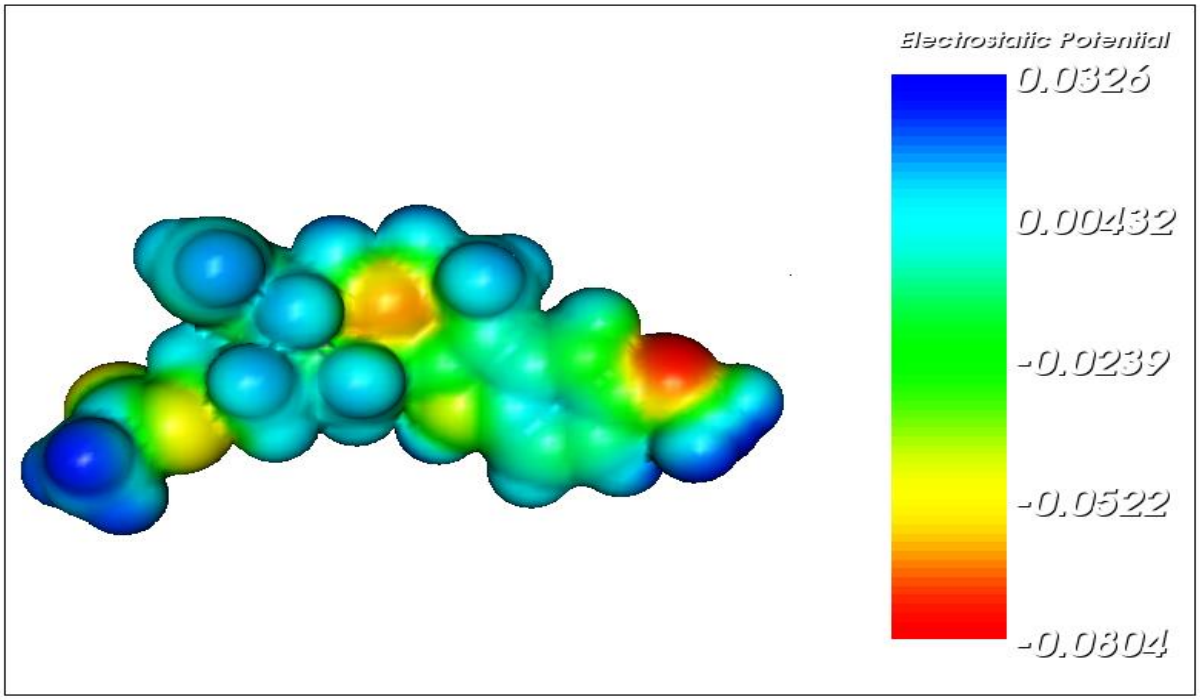

Fig. 4. Molecular electrostatic potential of corynan-17-ol, 18, 19-didehydro-10-methoxy, acetate..

8. Frontier molecular orbitals (FMOs)

The intramolecular HOMO and LUMO overlapping is important to predict the reactivity and stability of the molecule as the overlap between HOMO/LUMO is the most governing factor in many reactions.The HOMO (5.033057536) represent the ability to donate an electron and LUMO (0.092791556) as an electron acceptor represents the ability to achieve an electronare shown in **Fig. 5**. From the HOMO-LUMO(4.94026598) energy gap, we can see that whether or not the molecule was hard or softare listed in **Table 4**. If the molecule had large energy gap then the molecule can be called as hard molecule and presence of small energy gap makes the molecule as soft[13]. Softness is a measure of how easily the electron density can be distorted by external fields.The energy gap value reflects the properties of the molecule.

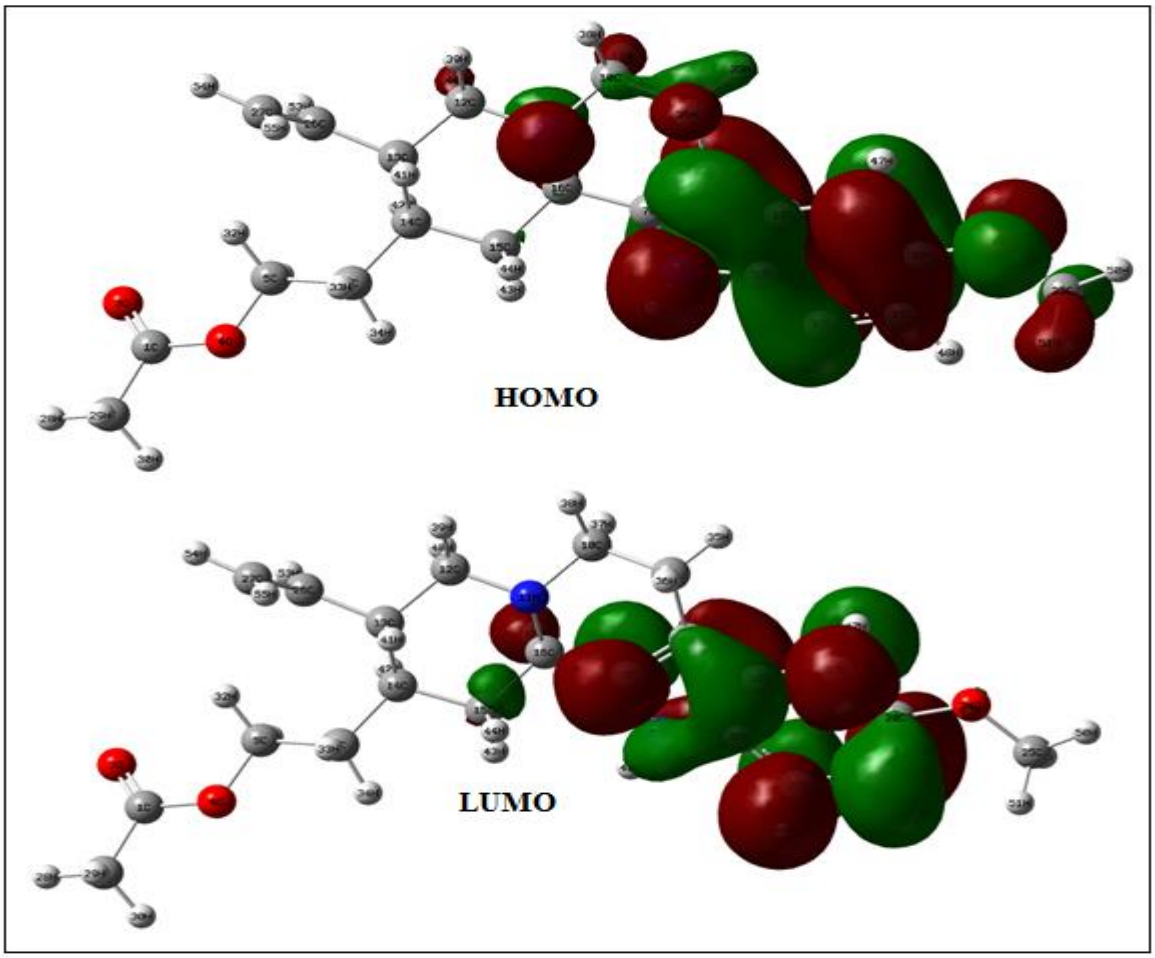

Fig. 5. The atomic orbital composition of the frontier molecular orbital of corynan-17-ol, 18, 19-didehydro-10-methoxy, acetate.

Table 4: Calculated energy values of corynan-17-ol, 18, 19-didehydro-10-methoxy, acetate by B3LYP/6-31++G(d,p) methods.

Molecular Properties	**B3LYP/6-31++G(d,p)**	**Molecular Properties**	**B3LYP/6-31++G(d,p)**
$E_{(HOMO)}$ (eV)	5.033057536	Chemical Hardness (η)	-2.470130988
$E_{(LUMO)}$ (eV)	0.092791556	Softness (s)	-0.40483683
$E_{(HOMO-LUMO)}$ gap (eV)	4.94026598	Chemical Potential (μ)	2.562924458
Ionisation Potential (I)	-5.033057536	Electron Affinity (χ)	-2.562924458
Electron Affinity (A)	-0.092791556	ElectronPhilicity Index (ω)	3.284290889

9. UV-Vis

The calculated excitation energies, oscillator strengths (f) and wavelengths (λ) are given in Table 5. Calculations of molecular orbital geometry show that the visible absorption maxima of this molecule correspond to the electron transition between frontier orbitals such as translation from HOMO to LUMO. The maximum absorption peak (λmax) observed in UV-Vis spectrum corresponds to vertical transitions according to Frank–Condon principle. Itcould be seen that low energy absorption found at 272 nm and 265nm belongs to the dipole allowed π–π^* and π – π^* transition from HOMO to LUMO, respectively. The λ_{max} is a function of substitution, the stronger the donor character of the substitution, the more electrons pushed into the molecule, the larger λ_{max} are shown in Fig. 6. As can be seen from Table 5, TD-DFT/6-311++G(d,p) method predicts two electronic transitions at λ_{cal} = 277.85 nm with f = 4.4623, λ_{cal}=270.82with f=4.4752 and λ_{cal}= 252.52 nm with f = 4.9097[14].

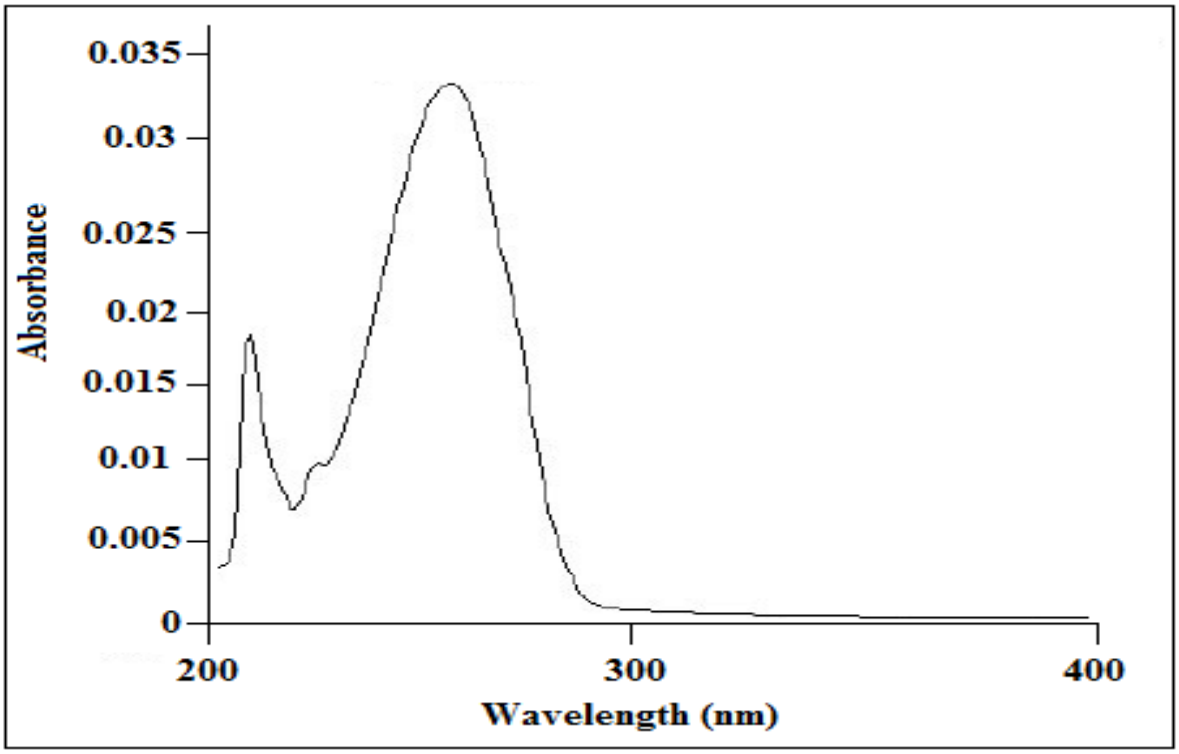

Fig. 6. UV–V is spectrum of corynan-17-ol, 18, 19-didehydro-10-methoxy, acetate.

Table 5: The UV–Vis excitation energy of corynan-17-ol, 18, 19-didehydro-10-methoxy, acetate.

States	Experimental	TD B3LYP/(6-31)++G(d,p)		
	Exp	Gas phase		
		λ_{call}	E(ev)	Oscillator Strengths(f)
S_1	272	277.85	4.4623	0.1523
S_2	265	270.82	4.4752	0.0090
S_3	-	252.53	4.9097	0.0002

10. NBO

NBO (Natural bond orbital) is used in computational chemistry to calculate bonds, bond order, donor-acceptor interactions and the distribution of electron density between atoms. The less negative charge of C_{27} and C_9 is due to the attachment of highly electronegative oxygen atoms O_{15} and O_{19} to it. The very high positive charge on the hydrogen atoms H_{46} and H_{29} is due to the difference in electronegativity of these atoms and oxygen atoms. The possible selective intra-molecular hyper conjugative interactions noticed in corynan-17-ol, 18, 19-didehydro-10-methoxy, acetate are σ *C_{18}-C_{23} $\rightarrow\pi^{*}C_{21}$-C_{22} ,$LP(2)O_4\rightarrow\pi^{*}C_1$-$O_3$, $\sigma^{*}C_{18}$-$C_{23}\rightarrow\pi^{*}C_7$-$C_8$, with stabilization energies 23.42, 49.88, 144.35Kcal/mol are listed in **Table 6**[15].

Table 6: Second-order perturbation theory analysis of Fock matrix in NBO basis corresponding to the intramolecular bonds of corynan-17-ol, 18, 19-didehydro-10-methoxy, acetate.

Donor NBO (i)	Acceptor NBO (j)	$E^{(2)a}$ (kJ/mol)	E(j)-E(i) (a.u)	F(i,j) (a.u)
$\sigma\ ^{*}C_7$-C_8	$\pi\ ^{*}C_{18}$-C_{23}	16.67	0.28	0.067
$\sigma\ ^{*}C_{18}$-C_{23}	$\pi\ C_7$-C_8	17.22	0.28	0.064
$\sigma\ ^{*}C_{18}$-C_{23}	$\pi\ ^{*}C_{19}$-C_{20}	19.70	0.24	0.065
$\sigma\ ^{*}C_{18}$-C_{23}	$\pi\ ^{*}C_{21}$-C_{22}	23.42	0.26	0.070
$\sigma\ ^{*}C_{19}$-C_{20}	$\pi\ C_{18}$-C_{23}	19.34	0.28	0.069
$\sigma\ ^{*}C_{19}$-C_{20}	$\pi\ C_{21}$-C_{22}	18.83	0.27	0.065
$\sigma\ ^{*}C_{21}$-C_{22}	$\pi\ ^{*}C_{18}$-C_{23}	17.11	0.28	0.066
$\sigma\ ^{*}C_{21}$-C_{22}	$\pi\ ^{*}C_{19}$-C_{20}	19.35	0.28	0.068
LP $(2)O_3$	$\pi\ C_1$-C_2	16.36	0.64	0.094
$LP(2)O_3$	$\pi\ C_1$-O_4	34.54	0.57	0.126
$LP(2)O_4$	$\pi\ ^{*}C_1$-O_3	49.88	0.30	0.109
LP $(1)\ N_{17}$	$\pi\ ^{*}C_7$-C_8	35.47	0.30	0.093
$LP(1)N_{17}$	$\pi\ ^{*}C_{18}$-C_{23}	31.74	0.29	0.089
LP $(2)\ O_{24}$	$\pi\ ^{*}C_{19}$-C_{20}	24.31	0.33	0.085
$\sigma\ ^{*}C_{18}$-C_{23}	$\pi\ ^{*}C_7$-C_8	144.35	0.01	0.064

11. Molecular Docking Studies (Procedure)

In the molecular docking studies, the three-dimensional X-ray structure of (Human serum Albumin) HSA (PDB code: 1AO6) was downloaded from protein data bank (http://www.pdb.org) and the structures of quinolizine derivative are sketched by CHEMSKETCH and converted into PDB format from mol format by OPENBABEL. Molecular docking studies have been done use Maestro-10.2 docking program inbuilt in schrodinger suite. Initially, in the protein preparation step assign bond orders to the protein residue followed by add polar hydrogens and removed water beyond 5Å. Finally, the protein structure was optimized by using force field (OPLS-2005) and their structure suitable for docking with quinolizine derivative. The energy calculations were made using genetic algorithms. The outputs were exported to PyMol for visual inspection of the binding modes and for possible polar and hydrophobic exchanges of the compounds with HAS[16].

To evaluate the binding affinity of the quinolizine derivatives with human serum albumin (HSA), the docking studies were carried out for using Maestro 10.2 docking program and the visualization of docking site and 3D interactions results obtained from the studies are given in **Fig.6 and.7.** The observed docking score value found to be 4.81kcal mol^{-1} which showed effective interaction between quinolizine derivatives and receptor. Moreover, the binding results suggested various mode of interaction via H-bond, π-π stacking, Van der Waals, and electrostatic interaction. The compound showing active mode of interaction with HSA receptor shows two hydrogen bond one with LYS 436 (distance 1.739Å) and other ASN 295(distance 1.753Å) and π-π stacking interaction with ARG 218 (distance 4.30Å). In addition, there were hydrophobic interaction with many amino acid residues: ALA 191, ALA 194, LEU 198, TRP 214, TYR 341, VAL 343, PRO 339, PRO 447 and CYS 448. The docking results showed better activity against receptor human serum albumin.

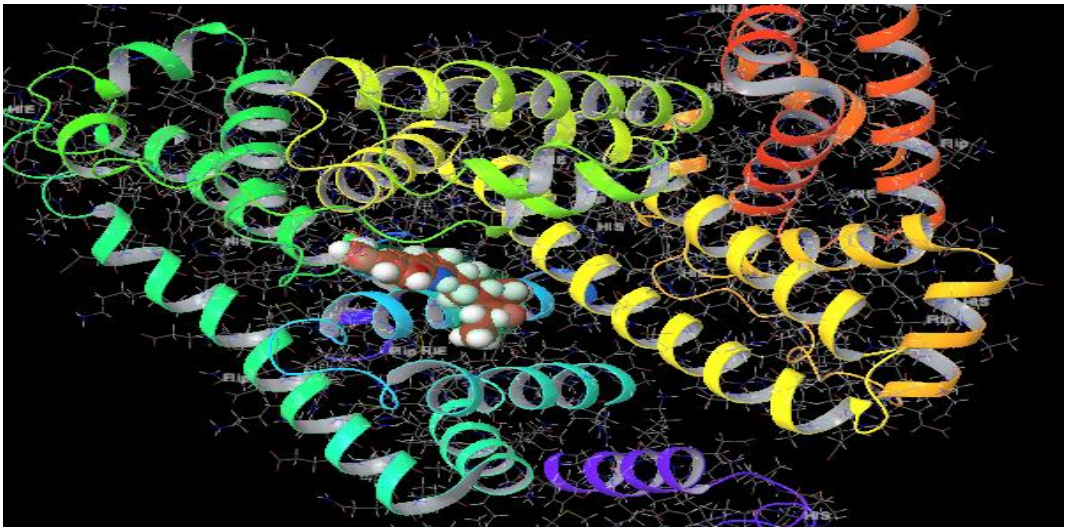

Fig 7. Molecular docking forces of quinolizine derivatives located in the active site of the HSA receptor

12. Conclusions

A comprehensive spectroscopy and theoretical study at density functional theory (DFT) was successfully achieved for a natural product, corynan-17-ol, 18, 19-didehydro-10-methoxy, acetate. corynan-17-ol, 18, 19-didehydro-10-methoxy, acetate was isolated from Cassia auriculata plant and then characterized with different experimental techniques such as IR and UV–Vis.The FT-IR spectra and DTF studies of corynan-17-ol, 18, 19-didehydro-10-methoxy, acetate were carried out for the first time.FT-IR vibrational spectra showed the characteristic functional groups of corynan-17-ol, 18, 19-didehydro-10-methoxy, acetate. The experimental and predicted FT-IR and UV–Vis spectra [B3LYP/6- 311++G(d,p)] have excellent correlation with minor exception, which can be attributed to the corynan-17-ol, 18, 19-didehydro-10-methoxy, acetate in the experiment.Which are responsible for the bioactive property of the biomedical compound corynan-17-ol, 18, 19-didehydro-10-methoxy, acetate.Results demonstrated that the nitrogen containing compound increased the antibacterial activity.The docking results showed better activity against receptor human serum albumin. Our theoretical results also corroborate to the experimental results.

References

[1] HaiderMashkoor Hussein, ImadHadiHameed ,Jenan Mohammed Ubaid.
International Journal of Pharmacognosy and Phytochemical Research 2016; 8(8); 1403-1411.
[2] S. Selvaraj , P. Rajkumar , M. Kesavan , K. Mohanraj , S. Gunasekaran , S. Kumaresan ,Chemical Data Collections 17–18 (2018) 302–311.
[3] AnamArain, Syed TufailHussainSherazi ,Sarfaraz Ahmed Mahesar, And Sirajuddin,International Journal Of Food Properties ,2017, Vol. 20, S556–S563
[4] M.J. Frisch , et al. , Gaussion 09W, Revision A.02, GaussionInc, Walling ford, CT, 2009 .
[5] P. Rajesh , S. Gunasekaran , T. Gnanasambandan , S. Seshadri,SpectrochimicaActa Part A: Molecular and Biomolecular Spectroscopy 137 (2015) 1184–1193.
[6]M.V.S. Prasad , N. Udaya Sri , V. Veeraiah, SpectrochimicaActa Part A: Molecular and Biomolecular Spectroscopy 148 (2015) 163–174.
[7]F. Bardak , C. Karaca , S. Bilgili , A. Atac , T.Mavis , A.M. Asiri , M. Karabacak, E. Kose,SpectrochimicaActa Part A: Molecular and Biomolecular Spectroscopy 165 (2016) 33–46.

[8]A. Nataraj , V. Balachandran , T. Karthick, Journal of Molecular Structure 1022 (2012) 94–108.
[9]M. Prabhaharana,b, A.R. Prabakaran b, S. Gunasekaran c, S. SrinivasanSpectrochimicaActa Part A: Molecular and Biomolecular Spectroscopy 123 (2014) 392–401.
[10] P. Rajesh , S. Gunasekaran , T. Gnanasambandan , S. Seshadri,SpectrochimicaActa Part A: Molecular and Biomolecular Spectroscopy 136 (2015) 247–255.
[11]P. Rajesh , S. Gunasekaran, T. Gnanasambandan , S. Seshadri,SpectrochimicaActa Part A: Molecular and Biomolecular Spectroscopy 153 (2016) 496–504.
[12] F. Bardak , C. Karaca , S. Bilgili , A. Atac , T.Mavis , A.M. Asiri , M. Karabacak, E. Kose,SpectrochimicaActa Part A: Molecular and Biomolecular Spectroscopy 165 (2016) 33–46.
[13]V. Mukherjee , T. Yadav,SpectrochimicaActa Part A: Molecular and Biomolecular Spectroscopy 165 (2016) 167–175.
[14] M. Karabacak , M. Cinar , M. Kurt , A. Poiyamozhi , N. Sundaraganesan,SpectrochimicaActa Part A: Molecular and Biomolecular Spectroscopy 117 (2014) 234–244.
[15] R. John Xavier , P. Dinesh, SpectrochimicaActa Part A: Molecular and Biomolecular Spectroscopy 136 (2015) 1569–1581.
[16]Sergio Abbate , Giovanna Longhi , France Lebon, MatteoTommasini,Chemical Physics 405 (2012) 197–205.

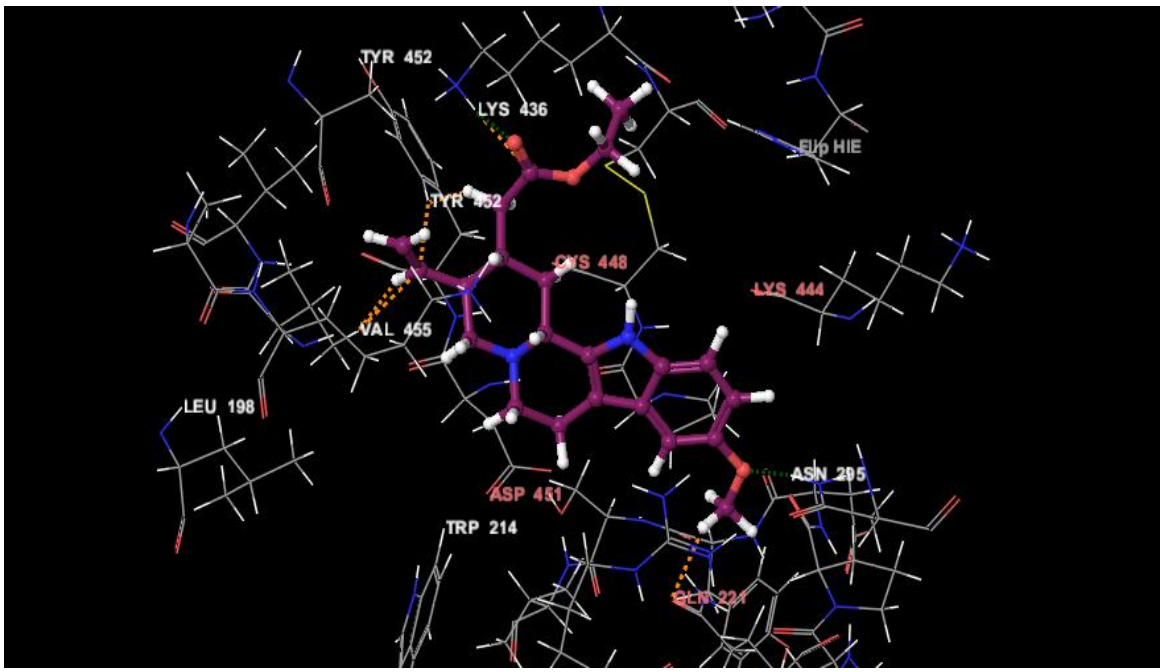

Fig 8. 3D interaction modes of quinolizine derivatives with HSA receptor